

Muon $g - 2$ in $U(1)_{\mu-\tau}$ Symmetric Gauged Radiative Neutrino Mass ModelDong Woo Kang,^{1,*} Jongkuk Kim,^{1,†} and Hiroshi Okada^{2,3,‡}¹*School of Physics, KIAS, Seoul 02455, Korea*²*Asia Pacific Center for Theoretical Physics (APCTP) - Headquarters San 31,**Hyoja-dong, Nam-gu, Pohang 790-784, Korea*³*Department of Physics, Pohang University of Science and Technology, Pohang 37673, Republic of Korea*

We explore muon anomalous magnetic moment (muon $g - 2$) in a scotogenic neutrino model with a gauged lepton number symmetry $U(1)_{\mu-\tau}$. In this model, a dominant muon $g - 2$ contribution comes not from an additional gauge sector but from a Yukawa sector. In our numerical $\Delta\chi^2$ analysis, we show that our model is in favor of normal hierarchy with some features. We demonstrate one benchmark point, satisfying muon $g - 2$ at the best fit value 25.1×10^{-10} .

PACS numbers:

arXiv:2107.09960v2 [hep-ph] 19 Sep 2021

*Electronic address: dongwookang@kias.re.kr

†Electronic address: jkkim@kias.re.kr

‡Electronic address: hiroshi.okada@apctp.org

I. INTRODUCTION

Flavor dependent gauged $U(1)$ scenarios; especially $U(1)_{\mu-\tau}$ [1, 2], are widely applied to explaining recent anomalies such as muon anomalous magnetic moment (muon $g - 2$ or Δa_μ) [3–16] and rare B meson decays $b \rightarrow s\ell\bar{\ell}$ [17–21] as beyond the Standard Model (SM), in addition to neutrino mass models [22–27].¹ In fact, the longstanding muon $g - 2$ anomaly was first discovered by BNL two decades ago and is recently confirmed by FNAL. Combined two results are given by [29]

$$\Delta a_\mu^{\text{new}} = (25.1 \pm 5.9) \times 10^{-10}. \quad (\text{I.1})$$

The deviation from the SM expectation is 4.2σ confidence level. One can typically address this deviation with the contribution from additional gauge boson with new neutral gauge boson mass $m_{Z'}$ and coupling g' . Even though there are several constraints on this new gauge sector such as neutrino trident bound; $m_{Z'}/g' \lesssim 550$ GeV, there exists allowed region [30].

In this paper, we propose a scotogenic neutrino model with $U(1)_{\mu-\tau}$ gauge symmetry that explains muon $g - 2$ by the Yukawa sectors not by the new gauge sector. In order to get the sizable muon $g - 2$, we need a diagram without chiral suppression and we introduce several exotic fermions and scalars. These several exotic fermions can also play a role in radiative neutrino mass generation at one-loop level [31]. Heavier neutral fermions run inside the loop and the lightest one could be a promising dark matter (DM) candidate. Finally, we show several features of our model by demonstrating the numerical $\Delta\chi^2$ analysis.

This paper is organized as follows. In Sec. II, we present the model set up and how to generate neutrino masses in normal and inverted hierarchy. In Sec. III, we discuss constraints from lepton flavor violations (LFVs) and address the muon anomalous magnetic moment. We carry out numerical $\Delta\chi^2$ analysis and present the allowed region satisfying the neutrino oscillation data, LFVs and muon $g - 2$. Conclusions and discussions are given in Sec. IV, briefly mentioning a possibility of DM candidate and how to explain the correct relic density, satisfying direct detection bounds.

II. MODEL

¹ Flavor dependent gauge $U(1)$ scenarios can modify the lepton universality, since a new gauge boson Z' does not universally couple to lepton sector. See [28].

	Leptons									
Fermions	L_{Le}	$L_{L\mu}$	$L_{L\tau}$	ℓ_{Re}	$\ell_{R\mu}$	$\ell_{R\tau}$	N_{Re}	$N_{R\mu}$	$N_{R\tau}$	L'
$SU(2)_L$	2	2	2	1	1	1	1	1	1	2
$U(1)_Y$	$-\frac{1}{2}$	$-\frac{1}{2}$	$-\frac{1}{2}$	-1	-1	-1	0	0	0	$-\frac{1}{2}$
$U(1)_{\mu-\tau}$	0	1	-1	0	1	-1	0	1	-1	0
Z_2	+	+	+	+	+	+	-	-	-	-

TABLE I: Field contents of fermions and their charge assignments under $SU(2)_L \times U(1)_Y \times U(1)_{\mu-\tau} \times Z_2$, where $SU(3)_C$ is singlet.

	VEV $\neq 0$		VEV = 0	
Bosons	H	φ	η	χ^-
$SU(2)_L$	2	1	2	1
$U(1)_Y$	$\frac{1}{2}$	0	$\frac{1}{2}$	-1
$U(1)_{\mu-\tau}$	0	1	0	1
Z_2	+	+	-	-

TABLE II: Field contents of bosons and their charge assignments under $SU(2)_L \times U(1)_Y \times U(1)' \times Z_2$, where $SU(3)_C$ is singlet.

In this section, we set up our model Lagrangian and focus on lepton sector and Higgs sector which are crucial for generating neutrino mass and muon g-2 contribution. And we address detail discussion for the neutrino mass matrix.

A. Lepton Lagrangian

We introduce three right-handed neutral fermions $[N_{Re}, N_{R\mu}, N_{R\tau}]$ with $[0, 1, -1]$ charges under $U(1)_{\mu-\tau}$ symmetry and an isospin doublet vector-like lepton $L' \equiv [N', E']^T$ with 0 under $U(1)_{\mu-\tau}$ symmetry. In addition, we impose Z_2 odd for new fermions where even is assigned to the SM fermions. The Z_2 symmetry plays a role in generating the active neutrino mass matrix not at tree-level but one-loop level. Furthermore, the lightest field with odd Z_2 can be a dark matter candidate. Notice here that the $U(1)_{\mu-\tau}$ anomaly is independently canceled among the SM fermions or N_R . In the bosonic sector, we introduce extra bosons with two isospin singlets φ, χ^- and a doublet η . These bosons respectively have $[1, 1, 0]$ charges under the $U(1)_{\mu-\tau}$ symmetry. φ is even under Z_2 and η, χ^- are odd under Z_2 and induce the active neutrino mass matrix together with N_R . The field contents and assignments for new fermions and the SM leptons are summarized in Tables I. Each of φ and the SM Higgs denoted by H has non-zero vacuum expectation values that are symbolized by $\langle \varphi \rangle \equiv$

$v_\varphi/\sqrt{2}$ and $\langle H \rangle \equiv [0, v_H/\sqrt{2}]^T$, after spontaneous symmetry breaking of $U(1)_{\mu-\tau}$ and electroweak symmetry. The bosonic field contents and their assignments are summarized in Tables II.

Under these symmetries, our renormalizable Lagrangian is given by

$$\begin{aligned}
-\mathcal{L}_Y = & M_{ee}\overline{N_{R_e}^c}N_{R_e} + M_{\mu\tau}(\overline{N_{R_\mu}^c}N_{R_\tau} + \overline{N_{R_\tau}^c}N_{R_\mu}) + M_{L'}\overline{L'_L}L'_R + \text{h.c.} \\
& + y_e\overline{L_{L_e}}He_R + y_\mu\overline{L_{L_\mu}}H\mu_R + y_\tau\overline{L_{L_\tau}}H\tau_R + \text{h.c.} \\
& + h_{e\mu}(\overline{N_{R_e}^c}N_{R_\mu} + \overline{N_{R_\mu}^c}N_{R_e})\varphi^* + h_{e\tau}(\overline{N_{R_e}^c}N_{R_\tau} + \overline{N_{R_\tau}^c}N_{R_e})\varphi + \text{h.c.} \\
& + f_e\overline{L_{L_e}}(i\sigma_2)\eta^*N_{R_e} + f_\mu\overline{L_{L_\mu}}(i\sigma_2)\eta^*N_{R_\mu} + f_\tau\overline{L_{L_\tau}}(i\sigma_2)\eta^*N_{R_\tau} \\
& + g_e\overline{\ell_{R_e}}N_{R_\mu}^c\chi^- + g_\mu\overline{\ell_{R_\mu}}N_{R_e}^c\chi^- \\
& + h\overline{L_{L_\mu}}L_{L'}^c\chi^- + y'\overline{L'_L}(i\sigma_2)H^*N_{R_e} + y''\overline{L'_R}HN_{R_e} + \text{h.c.}, \tag{II.1}
\end{aligned}$$

where σ_2 is the second Pauli matrix and the charged-lepton mass matrix is diagonal due to the $\mu-\tau$ symmetry; $\mathcal{M}_\ell = \frac{v_H}{\sqrt{2}}\text{diag}(|y_e|, |y_\mu|, |y_\tau|) \equiv (m_e, m_\mu, m_\tau)$ after the phase redefinition. Therefore, the neutrino oscillation data is induced via neutrino sector.

B. Higgs sector

Our Higgs potential is also given by

$$\mathcal{V} = \mathcal{V}_2^{tri} + \mathcal{V}_4^{tri} + \lambda_0(H^\dagger\eta)^2 + \lambda'_0\varphi^*(H^T i\sigma_2\eta)\chi^- + \text{h.c.}, \tag{II.2}$$

where we define $\eta \equiv [\eta^+, (\eta_R + i\eta_I)/\sqrt{2}]^T$, $H \equiv [h^+, (v_H + h_0 + iz_0)/\sqrt{2}]^T$, $\varphi \equiv (v_\varphi + \varphi_R + iz_\varphi)/\sqrt{2}$, and \mathcal{V}_2^{tri} and \mathcal{V}_4^{tri} are respectively trivial quadratic and quartic terms of the Higgs potential; $\mathcal{V}_2^{tri} = \sum_{\phi=H,\varphi,\eta,\chi^-} \mu_\phi^2|\phi|^2$, $\mathcal{V}_4^{tri} = \sum_{\phi'\leq\phi}^{H,\varphi,\eta,\chi^-} \lambda_{\phi\phi'}|\phi|^2|\phi'|^2 + \lambda'_{H\eta}|H^\dagger\eta|^2$. Notice here that h^+ , z_0 , and z_φ are respectively absorbed by the longitudinal degrees of freedom in gauge sectors. Consequently, we have massive gauge bosons W^\pm, Z in the SM and Z' in the $U(1)_{\mu-\tau}$ gauge symmetry. The λ_0 term plays an important role in generating the non-vanishing neutrino mass matrix. In our model, the neutrino mass matrix is proportional to the mass-squared difference between η_R and η_I ; $m_R^2 - m_I^2 = \lambda_0 v_H^2$, where $m_{R,I}$ is the mass eigenstate of $\eta_{R,I}$ [31]. Even though there is mixing between χ^\pm and η^\pm from λ'_0 , we suppose that the mixing is negligibly tiny.²

² If we consider the large mixing, we have a contribution to muon $g-2$ without chiral suppression, which might lead to large muon $g-2$. However, it cannot be large enough. In fact, we need large mass hierarchy between them, but it is forbidden by oblique parameters [32]. Satisfying these conditions, we have found $\Delta a_\mu \approx 10^{-13}$ at most in our numerical estimation.

C. Neutral fermion mass matrices

After the phase redefinition of the neutral fermions, the mass matrix in basis of $[N_{R_e}, N_{R_\mu}, N_{R_\tau}, N_L^c, N_R']$ is found as follows:

$$\mathcal{M}_N = \begin{pmatrix} M_{ee} & M_{e\mu} & M_{e\tau} & m' & m''e^{i\zeta} \\ M_{e\mu} & 0 & M_{\mu\tau}e^{i\xi} & 0 & 0 \\ M_{e\tau} & M_{\mu\tau}e^{i\xi} & 0 & 0 & 0 \\ m' & 0 & 0 & 0 & M_{L'} \\ m''e^{i\zeta} & 0 & 0 & M_{L'} & 0 \end{pmatrix}, \quad (\text{II.3})$$

where $M_{e\mu} \equiv \frac{v_\varphi}{\sqrt{2}}|h_{e\mu}|$, $M_{e\tau} \equiv \frac{v_\varphi}{\sqrt{2}}|h_{e\tau}|$, $m' \equiv \frac{v_H}{\sqrt{2}}|y'|$, $m'' \equiv \frac{v_H}{\sqrt{2}}|y''|$ are real mass parameters, while ξ , ζ are physical phases. The mass matrix \mathcal{M}_N is then diagonalized by introducing a unitary matrix V . This matrix satisfies

$$V^T \mathcal{M}_N V \equiv \text{diag}(M_1, M_2, M_3, M_4, M_5). \quad (\text{II.4})$$

Here, the mass eigenstate ψ_R is defined by $N_{R_i} = \sum_{k=1}^5 V_{ik} \psi_{R_k}$, and its mass eigenvalue is defined by $M_k (k = 1, 2, 3, 4, 5)$. Then, the valid Lagrangian is rewritten in terms of mass eigenstates as follows³:

$$-\mathcal{L} = \bar{\nu}_{L_a} F_{ak} \psi_{R_k} (\eta_R - i\eta_I) - \sqrt{2} \bar{\ell}_{L_a} F_{ak} \psi_{R_k} \eta^- + \bar{\ell}_{R_{a'}} G_{a'k} \psi_{R_k}^C \chi^- + H_{4k} \bar{\mu}_L \psi_{R_k} \chi^- + \text{h.c.}, \quad (\text{II.5})$$

$$F_{ia} = \frac{1}{\sqrt{2}} \sum_{j=1,2,3} \begin{pmatrix} f_e & 0 & 0 \\ 0 & f_\mu & 0 \\ 0 & 0 & f_\tau \end{pmatrix}_{ij} V_{ja}, \quad G_{ia} = \sum_{j=1,2,3} \begin{pmatrix} 0 & g_e & 0 \\ g_\mu & 0 & 0 \end{pmatrix}_{ij} V_{ja}^*, \quad H_{4k} \equiv h \sum_{k=1}^5 V_{4k}, \quad (\text{II.6})$$

where F is three by five matrix, and G is two by five matrix, therefore a' runs over e, μ . The first term of Eq. (II.5) contributes to the neutrino mass matrix, while the other terms induce LFVs, and muon $g-2$ as can be seen below. The active neutrino mass matrix is given by [31]

$$\begin{aligned} (m_\nu)_{ij} &= \sum_{k=1}^5 \frac{F_{ik} M_k F_{kj}^T}{2(4\pi)^2} \left[\frac{m_R^2}{m_R^2 - M_k^2} \ln \frac{m_R^2}{M_k^2} - \frac{m_I^2}{m_I^2 - M_k^2} \ln \frac{m_I^2}{M_k^2} \right] \\ &\simeq \frac{\lambda_0 v_H^2}{(4\pi)^2} \sum_{k=1}^5 \frac{F_{ik} M_k F_{kj}^T}{m_0^2 - M_k^2} \left[1 - \frac{M_k^2}{m_0^2 - M_k^2} \ln \frac{m_0^2}{M_k^2} \right], \end{aligned} \quad (\text{II.7})$$

where we assume to be $\lambda_0 v_H^2 = m_R^2 - m_I^2 \ll m_0^2 \equiv (m_R^2 + m_I^2)/2$ in the second line, and m_ν is diagonalized by a unitary matrix U_{PMNS} [33]; $D_\nu \equiv U_{\text{PMNS}}^T m_\nu U_{\text{PMNS}}$. Here, we define dimensionless

³ Notice here that $h \bar{\nu}_{\mu L} E_L^c \chi^-$ does not contribute to the neutrino mass matrix, since E_L^c cannot propagate in the loop.

neutrino mass matrix as $m_\nu \equiv (\lambda_0 v_H) \tilde{m}_\nu \equiv \kappa \tilde{m}_\nu$. Since κ does not depend on the flavor structure, we rewrite this diagonalization in terms of dimensionless form $(\tilde{D}_{\nu_1}, \tilde{D}_{\nu_2}, \tilde{D}_{\nu_3}) \equiv U_{\text{PMNS}}^T \tilde{m}_\nu U_{\text{PMNS}}$. Thus, we fix κ by

$$(\text{NH}) : \kappa^2 = \frac{|\Delta m_{\text{atm}}^2|}{\tilde{D}_{\nu_3}^2 - \tilde{D}_{\nu_1}^2}, \quad (\text{IH}) : \kappa^2 = \frac{|\Delta m_{\text{atm}}^2|}{\tilde{D}_{\nu_2}^2 - \tilde{D}_{\nu_3}^2}, \quad (\text{II.8})$$

where Δm_{atm}^2 is the atmospheric neutrino mass-squared difference. Here, NH and IH stand for the normal hierarchy and the inverted hierarchy, respectively. Subsequently, the solar neutrino mass-squared difference is depicted in terms of κ as follows:

$$\Delta m_{\text{sol}}^2 = \kappa^2 (\tilde{D}_{\nu_2}^2 - \tilde{D}_{\nu_1}^2). \quad (\text{II.9})$$

This should be within the experimental value. The neutrinoless double beta decay is also given by

$$\langle m_{ee} \rangle = \kappa \left| \tilde{D}_{\nu_1} \cos^2 \theta_{12} \cos^2 \theta_{13} + \tilde{D}_{\nu_2} \sin^2 \theta_{12} \cos^2 \theta_{13} e^{i\alpha_2} + \tilde{D}_{\nu_3} \sin^2 \theta_{13} e^{i(\alpha_3 - 2\delta_{CP})} \right|, \quad (\text{II.10})$$

which may be able to be observed by KamLAND-Zen in future [34].

III. RESULTS

A. Lepton flavor violations

Because of the flavor dependence in Eq.(II.5), we have lepton flavor violation decay processes for example, $\mu \rightarrow e\gamma$ or $\bar{\mu} \rightarrow \bar{e}\gamma$. These decay channels are originated from the terms of GH^\dagger or HG^\dagger .⁴ The corresponding branching ratio is given as follows [35–37]

$$\text{BR}(\bar{\mu} \rightarrow \bar{e}\gamma) \simeq \frac{48\pi^3 \alpha_{\text{em}}}{(4\pi)^4 m_{\ell_i}^2 G_F^2} |H_{4k} M_k G_{k1}^\dagger F(M_k, m_\chi)|^2, \quad (\text{III.1})$$

$$\text{BR}(\mu \rightarrow e\gamma) \simeq \frac{48\pi^3 \alpha_{\text{em}}}{(4\pi)^4 m_{\ell_i}^2 G_F^2} |G_{1k} M_k H_{k4}^\dagger F(M_k, m_\chi)|^2, \quad (\text{III.2})$$

$$F(m_1, m_2) = \int [dx]_3 \frac{y}{(x^2 - x)m_\mu^2 + xm_1^2 + (y+x)m_2^2}, \quad (\text{III.3})$$

where the fine structure constant $\alpha_{\text{em}} \simeq 1/135$ at muon mass energy scale [39], and the Fermi constant $G_F \simeq 1.17 \times 10^{-5} \text{ GeV}^{-2}$. The current experimental upper bound at 90% C.L. are [39, 40]

$$\text{BR}(\mu \rightarrow e\gamma) = \text{BR}(\bar{\mu} \rightarrow \bar{e}\gamma) < 4.2 \times 10^{-13}. \quad (\text{III.4})$$

⁴ In our numerical analysis, we also have considered non-dominant contributions of GG^\dagger and FF^\dagger .

B. Muon anomalous magnetic moment

In our model, we can achieve the required muon $g-2$ contribution through the same interaction with LFVs. The muon $g-2$ contribution is given as

$$\Delta a_\mu \approx -\frac{m_\mu}{(4\pi)^2} \text{Re}[(H_{4k} M_k G_{k2}^\dagger + G_{2k} M_k H_{k4}^\dagger) F(M_k, m_\chi)] = -\frac{2m_\mu}{(4\pi)^2} \text{Re}[H_{4k} M_k G_{k2}^\dagger] F(M_k, m_\chi). \quad (\text{III.5})$$

Recent experimental estimation [41] of muon $g-2$ indicates the following value at 4.2σ [29]:

$$\Delta a_\mu = a_\mu^{\text{EXP}} - a_\mu^{\text{SM}} = (25.1 \pm 5.9) \times 10^{-10}. \quad (\text{III.6})$$

We fix the best fit (BF) value; $\Delta a_\mu = 25.1 \times 10^{-10}$, in our numerical analysis below.

C. Numerical analysis

We show our numerical $\Delta\chi^2$ analysis to satisfy the neutrino oscillation data, LFV ($\mu \rightarrow e\gamma$ only in our case) as well as muon $g-2$. Here we fix Δa_μ as BF value 25.1×10^{-10} , where we adopt five known observables $\sin^2 \theta_{12}$, $\sin^2 \theta_{23}$, $\sin^2 \theta_{13}$, Δm_{atm}^2 , Δm_{sol}^2 in Nufit 5.0 [42] at 3σ confidence level. Notice that we do not include the Dirac CP phase in $\Delta\chi^2$ analysis because of big ambiguity at 3σ interval. Furthermore, we employ Gaussian approximations for charged-lepton masses. However since we have found the allowed region within $4.59 \lesssim \sqrt{\Delta\chi^2}$ in case of IH, it does not satisfy the sizable muon $g-2$ whose maximum order is 10^{-12} in our model. Thus, we focus on NH only. At first, we fix the range of our input parameters as follows:

$$\{f_e, f_\mu, f_\tau\} \in [10^{-5}, 10], \quad \{h, |g_\mu|\} \in [1, 10], \quad \{\xi, \zeta\} \in [0, \pi], \quad \{m', m''\} \in [1, 617] \text{ GeV}, \quad (\text{III.7})$$

$$\{M_{ee}, M_{e\mu}, M_{e\tau}, M_{\mu\tau}\} \in [10, 10^6] \text{ GeV}, \quad \{m_{\eta^\pm}, M_{L'}, m_{\chi^\pm}, m_0\} \in [10^2, 10^6] \text{ GeV}, \quad (\text{III.8})$$

where $0.9 \times m_0 \leq m_{\eta^\pm} \leq 1.2 \times m_0$ to evade the bound on oblique parameters, and $g_e = 0$ to suppress the LFVs in our work.⁵ The upper bounds on m' , m'' come from $|y'(\prime\prime)| v_H / \sqrt{2}$ taking the limit of perturbation $|y'(\prime\prime)| = \sqrt{4\pi}$ in addition to $\{F, G, H\} \in \sqrt{4\pi}$.

In Fig. 1, we show the scatter plots of sum of neutrino masses $\sum m_i$ in terms of $\sin^2 \theta_{23}$ (left), neutrinoless double beta decay $\langle m_{ee} \rangle$ in terms of $\sin^2 \theta_{23}$ (center), and $\langle m_{ee} \rangle$ in terms of $\sum m_i$ (right). Here, each of the color plots of green, yellow, and red represents the region at σ of 0–1,

⁵ In the case of $g_e = 0$, both $\text{BR}(\mu \rightarrow e\gamma)$ and muon $g-2$ are proportional to $\text{Re}[hg_\mu^*]$ that does not depend on the flavor structure. Thus, we can take any values for h and g_μ in our numerical ranges as far as $\text{Re}[hg_\mu^*]$ does not change. In our benchmark points in Table III, we set h and g_μ as one of examples so as to be $\text{Re}[hg_\mu^*] \sim 1.52$.

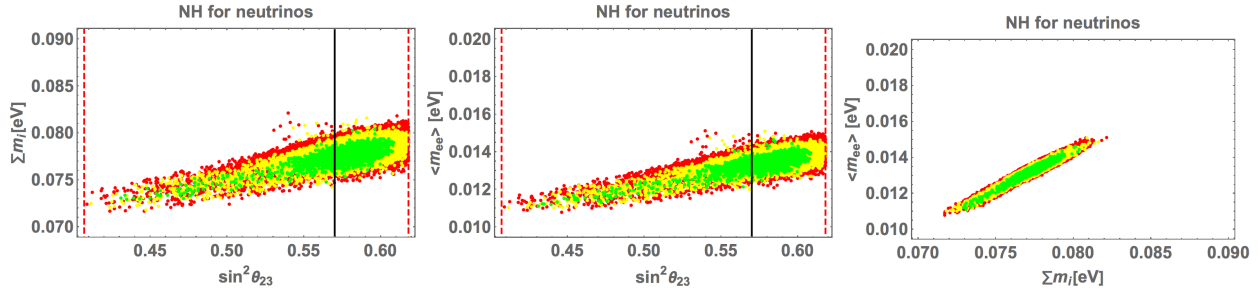


FIG. 1: The scatter plots of sum of the neutrino masses $\sum m_i$ in terms of $\sin^2 \theta_{23}$ (left), neutrinoless double beta decay $\langle m_{ee} \rangle$ in terms of $\sin^2 \theta_{23}$ (center), and $\langle m_{ee} \rangle$ in terms of $\sum m_i$ (right). Each of the color plots of green, yellow, and red represents the region at σ of 0–1, 1–2, 2–3, respectively. The each vertical line of black-solid and red-dotted represents the best fit and 3σ interval.

1–2, 2–3, respectively. After the $\Delta\chi^2$ analysis, as shown in the figure, we find that $\sum m_i$ is allowed in the range of [72.9 – 80.4] [meV] at 1σ interval, [71.8 – 81.6] [meV] at 2σ interval, [71.7 – 82.1] [meV] at 3σ interval. $\langle m_{ee} \rangle$ is allowed in the range of [11.1 – 14.6] [meV] at 1σ interval, [11.0 – 15.1] [meV] at 2σ interval, and [10.8 – 15.1] [meV] at 3σ interval.

Finally, we show a benchmark point for NH in Table III, where it is taken such that $\Delta\chi^2$ is minimum in our model. Notice here that all the phases δ_{CP} , α_{21} , α_{31} are very close to be zero through our $\sqrt{\Delta\chi^2}$ analysis.

IV. CONCLUSIONS AND DISCUSSIONS

We have proposed a gauged $U(1)_{\mu-\tau}$ neutrino mass model which can address the muon $g-2$ through the Yukawa sector without relying on the new gauge sector. The neutrino mass matrix is induced at one-loop level and participated in five neutral fermions run inside the loop. Through our numerical $\Delta\chi^2$ analysis, we have found that NH is in favor of our model. The best fit value of Δa_μ is mainly obtained by $\text{Re}[hg_\mu^*]$ in case of $g_e = 0$ for NH. IH does not satisfy the sizable muon $g-2$, but we have allowed region at $4.59 \lesssim \sqrt{\Delta\chi^2}$ in neutrino oscillation data. Several unique features are listed below:

1. $\sum m_i$ is allowed in the range of [72.9 – 80.4] [meV] at 1σ interval, [71.8 – 81.6] [meV] at 2σ interval, [71.7 – 82.1] [meV] at 3σ interval.
2. $\langle m_{ee} \rangle$ is allowed in the range of [11.1 – 14.6] [meV] at 1σ interval, [11.0 – 15.1] [meV] at 2σ interval, and [10.8 – 15.1] [meV] at 3σ interval.
3. All the phases δ_{CP} , α_{21} , α_{31} are localized in vicinity of zero through our $\Delta\chi^2$ analysis.

	NH
h	-1.005
g_μ	$1.514 + 0.628i$
$[f_e, f_\mu, f_\tau]$	$[14.5, -7.78, -17.7] \times 10^{-5}$
$[\xi, \zeta]$	$[328^\circ, 209^\circ]$
$[m_0, m_{\chi^\pm}, m_{\eta^\pm},]$	$[123, 165, 102] \text{ GeV}$
$\begin{pmatrix} M_{ee} & M_{e\mu} & M_{e\tau} & m' & m'' \\ M_{e\mu} & 0 & M_{\mu\tau} & 0 & 0 \\ M_{e\tau} & M_{\mu\tau} & 0 & 0 & 0 \\ m' & 0 & 0 & 0 & M_{L'} \\ m'' & 0 & 0 & M_{L'} & 0 \end{pmatrix}$	$\begin{pmatrix} 40.2 & 2.15 \times 10^4 & 8.12 \times 10^4 & 587 & -88.5 \\ 2.15 \times 10^4 & 0 & 8.34 \times 10^3 & 0 & 0 \\ 8.12 \times 10^4 & 8.34 \times 10^3 & 0 & 0 & 0 \\ 587 & 0 & 0 & 0 & 486 \\ -88.5 & 0 & 0 & 486 & 0 \end{pmatrix} \text{ GeV}$
$\text{BR}(\mu \rightarrow e\gamma)$	4.11×10^{-22}
Δm_{atm}^2	$2.52 \times 10^{-3} \text{ eV}^2$
Δm_{sol}^2	$7.44 \times 10^{-5} \text{ eV}^2$
$\sin^2 \theta_{12}$	0.307
$\sin^2 \theta_{23}$	0.573
$\sin^2 \theta_{13}$	0.0221
$[\delta_{CP}^\ell, \alpha_{21}, \alpha_{31}]$	$[0.191^\circ, 360^\circ, 0.405^\circ]$
$\sum m_i$	77.5 meV
$\langle m_{ee} \rangle$	13.3 meV
κ	5.33 GeV
$\sqrt{\Delta\chi^2}$	0.391

TABLE III: Numerical benchmark points of our input parameters and observables in NH, satisfying muon $g-2$ at the best fit value 25.1×10^{-10} . Here, the NH is taken such that $\sqrt{\Delta\chi^2}$ should be minimum.

Before closing our discussion, we briefly mention a DM candidate. Basically, we have two candidates; bosonic and fermionic one.

In case of bosonic DM candidate, the lightest particle of η_R and η_I is the one. *In case of fermionic DM candidate*, ψ_{R_1} is the one. In the case of fermionic DM candidate, we do not need to consider the bound on direct detection, because it does not interact with quark sector directly. The dominant cross section arises from G and H terms that also appear in muon $g-2$ and have s-wave dominant. But this contribution is at most $\mathcal{O}(5 \times 10^{-12}) \text{ GeV}^{-2}$ that is too small to resolve the correct relic density. Thus, our promising DM candidate is bosonic. Here, let us suppose η_R to be DM, and we simply neglect any interactions coming from Higgs potential in order to evade any bounds from

direct detection experiments.⁶ Moreover, we assume that the mass difference between η_R and η_I is more than 200 keV in order to evade the inelastic direct detection bounds via Z boson portal [43]. Similar to the result of fermionic case, we cannot rely on any contributions from Yukawa couplings because these contributions are too tiny to explain the relic density. Thus, we have to make the use of kinetic interactions from the SM. In this situation, nature of the DM is seriously analyzed by e.g. Ref. [45]. The solutions are uniquely found at the points of half of the Higgs mass; ~ 63 GeV and 534 GeV where coannihilation processes such as $\eta_R\eta_I \rightarrow Z \rightarrow \bar{f}f$ are taken in consideration.

Acknowledgments The work is supported in part by KIAS Individual Grants, Grant No. PG074202 (JK) and No. PG076201 (DK) at Korea Institute for Advanced Study. This research was supported by an appointment to the JRG Program at the APCTP through the Science and Technology Promotion Fund and Lottery Fund of the Korean Government. This was also supported by the Korean Local Governments - Gyeongsangbuk-do Province and Pohang City (H.O.). H.O. is sincerely grateful for all the KIAS members.

-
- [1] X. G. He, G. C. Joshi, H. Lew and R. R. Volkas, Phys. Rev. D **43**, 22-24 (1991) doi:10.1103/PhysRevD.43.R22
 - [2] X. G. He, G. C. Joshi, H. Lew and R. R. Volkas, Phys. Rev. D **44**, 2118-2132 (1991) doi:10.1103/PhysRevD.44.2118
 - [3] M. Davier, A. Hoecker, B. Malaescu and Z. Zhang, Eur. Phys. J. C **71**, 1515 (2011) [erratum: Eur. Phys. J. C **72**, 1874 (2012)] [arXiv:1010.4180 [hep-ph]].
 - [4] M. Davier, A. Hoecker, B. Malaescu and Z. Zhang, Eur. Phys. J. C **77**, no.12, 827 (2017) [arXiv:1706.09436 [hep-ph]].
 - [5] M. Davier, A. Hoecker, B. Malaescu and Z. Zhang, Eur. Phys. J. C **80**, no.3, 241 (2020) [erratum: Eur. Phys. J. C **80**, no.5, 410 (2020)] [arXiv:1908.00921 [hep-ph]].
 - [6] D. Borah, A. Dasgupta and D. Mahanta, [arXiv:2106.14410 [hep-ph]].
 - [7] X. Qi, A. Yang, W. Liu and H. Sun, [arXiv:2106.14134 [hep-ph]].
 - [8] S. Singirala, S. Sahoo and R. Mohanta, [arXiv:2106.03735 [hep-ph]].
 - [9] A. J. Buras, A. Crivellin, F. Kirk, C. A. Manzari and M. Montull, JHEP **06** (2021), 068 [arXiv:2104.07680 [hep-ph]].

⁶ This assumption would be reasonable since these couplings are highly suppressed by bound on direct detection searches. The coupling among DM and Higgses are of the order 10^{-3} [46].

- [10] S. Zhou, [arXiv:2104.06858 [hep-ph]].
- [11] D. Borah, M. Dutta, S. Mahapatra and N. Sahu, [arXiv:2104.05656 [hep-ph]].
- [12] J. Chen, Q. Wen, F. Xu and M. Zhang, [arXiv:2104.03699 [hep-ph]].
- [13] L. Zu, X. Pan, L. Feng, Q. Yuan and Y. Z. Fan, [arXiv:2104.03340 [hep-ph]].
- [14] G. y. Huang, F. S. Queiroz and W. Rodejohann, Phys. Rev. D **103** (2021) no.9, 095005 [arXiv:2101.04956 [hep-ph]].
- [15] S. Patra, S. Rao, N. Sahoo and N. Sahu, Nucl. Phys. B **917**, 317-336 (2017) [arXiv:1607.04046 [hep-ph]].
- [16] W. Altmannshofer, M. Carena and A. Crivellin, Phys. Rev. D **94**, no.9, 095026 (2016) [arXiv:1604.08221 [hep-ph]].
- [17] A. Crivellin, G. D'Ambrosio and J. Heeck, Phys. Rev. Lett. **114**, 151801 (2015) [arXiv:1501.00993 [hep-ph]].
- [18] A. Crivellin, G. D'Ambrosio and J. Heeck, Phys. Rev. D **91**, no.7, 075006 (2015) [arXiv:1503.03477 [hep-ph]].
- [19] J. Y. Cen, Y. Cheng, X. G. He and J. Sun, [arXiv:2104.05006 [hep-ph]].
- [20] P. Ko, T. Nomura and H. Okada, Phys. Rev. D **95** (2017) no.11, 111701 [arXiv:1702.02699 [hep-ph]].
- [21] N. Kumar, T. Nomura and H. Okada, [arXiv:2002.12218 [hep-ph]].
- [22] S. Baek, H. Okada and K. Yagyu, JHEP **04** (2015), 049 [arXiv:1501.01530 [hep-ph]].
- [23] T. Nomura and H. Okada, Phys. Lett. B **783** (2018), 381-386 [arXiv:1805.03942 [hep-ph]].
- [24] T. Nomura and H. Okada, Phys. Rev. D **97** (2018) no.9, 095023 [arXiv:1803.04795 [hep-ph]].
- [25] K. Asai, K. Hamaguchi, N. Nagata, S. Y. Tseng and K. Tsumura, Phys. Rev. D **99** (2019) no.5, 055029 [arXiv:1811.07571 [hep-ph]].
- [26] K. Asai, K. Hamaguchi and N. Nagata, Eur. Phys. J. C **77** (2017) no.11, 763 [arXiv:1705.00419 [hep-ph]].
- [27] S. Lee, T. Nomura and H. Okada, Nucl. Phys. B **931** (2018), 179-191 [arXiv:1702.03733 [hep-ph]].
- [28] E. J. Chun, A. Das, J. Kim and J. Kim, JHEP **02**, 093 (2019) [erratum: JHEP **07**, 024 (2019)] [arXiv:1811.04320 [hep-ph]].
- [29] B. Abi *et al.* [Muon g-2], Phys. Rev. Lett. **126** (2021) no.14, 141801 [arXiv:2104.03281 [hep-ex]].
- [30] W. Altmannshofer, S. Gori, M. Pospelov and I. Yavin, Phys. Rev. Lett. **113** (2014), 091801 [arXiv:1406.2332 [hep-ph]].
- [31] E. Ma, Phys. Rev. D **73** (2006), 077301 [arXiv:hep-ph/0601225 [hep-ph]].
- [32] M. E. Peskin and T. Takeuchi, Phys. Rev. D **46** (1992), 381-409
- [33] Z. Maki, M. Nakagawa and S. Sakata, Prog. Theor. Phys. **28** (1962), 870-880
- [34] A. Gando *et al.* [KamLAND-Zen], Phys. Rev. Lett. **117** (2016) no.8, 082503 [arXiv:1605.02889 [hep-ex]].
- [35] M. Lindner, M. Platscher and F. S. Queiroz, Phys. Rept. **731** (2018), 1-82 [arXiv:1610.06587 [hep-ph]].
- [36] A. E. Cárcamo Hernández, S. F. King, H. Lee and S. J. Rowley, Phys. Rev. D **101** (2020) no.11, 115016 [arXiv:1910.10734 [hep-ph]].
- [37] S. Baek, T. Nomura and H. Okada, Phys. Lett. B **759** (2016), 91-98 [arXiv:1604.03738 [hep-ph]].

- [38] J. Erler, Phys. Rev. D **59**, 054008 (1999) [arXiv:hep-ph/9803453 [hep-ph]].
- [39] A. M. Baldini *et al.* [MEG], Eur. Phys. J. C **76** (2016) no.8, 434 [arXiv:1605.05081 [hep-ex]].
- [40] J. Adam *et al.* [MEG], Phys. Rev. Lett. **110** (2013), 201801 [arXiv:1303.0754 [hep-ex]].
- [41] D. Hanneke, S. Fogwell and G. Gabrielse, Phys. Rev. Lett. **100** (2008), 120801 [arXiv:0801.1134 [physics.atom-ph]].
- [42] I. Esteban, M. C. Gonzalez-Garcia, M. Maltoni, T. Schwetz and A. Zhou, JHEP **09** (2020), 178 [arXiv:2007.14792 [hep-ph]].
- [43] R. Barbieri, L. J. Hall and V. S. Rychkov, Phys. Rev. D **74** (2006), 015007 [arXiv:hep-ph/0603188 [hep-ph]].
- [44] P. A. R. Ade *et al.* [Planck], Astron. Astrophys. **571** (2014), A16 [arXiv:1303.5076 [astro-ph.CO]].
- [45] T. Hambye, F. S. Ling, L. Lopez Honorez and J. Rocher, JHEP **07** (2009), 090 [erratum: JHEP **05** (2010), 066] [arXiv:0903.4010 [hep-ph]].
- [46] S. Kanemura, S. Matsumoto, T. Nabeshima and N. Okada, Phys. Rev. D **82** (2010), 055026 [arXiv:1005.5651 [hep-ph]].